ChemComm

COMMUNICATION

View Article Online
View Journal | View Issue

Cite this: *Chem. Commun.*, 2014, **50**, 5336

Received 28th September 2013,
Accepted 17th October 2013

DOI: 10.1039/c3cc47427e

www.rsc.org/chemcomm

Multifunctional squalene-based prodrug nanoparticles for targeted cancer therapy†

Duc Trung Bui, Julien Nicolas,* Andrei Maksimenko, Didier Desmaële and Patrick Couvreur

Fluorescent and biotinylated squalene–gemcitabine prodrug nanoparticles exhibiting high drug payloads have been prepared and successfully used to target different cancer cell lines, resulting in increased cell uptake and improved anticancer efficiency, which represents the first targeted system derived from the squalenoylation approach.

The medical application of nanotechnology, often termed nanomedicine, has witnessed a crucial step forward with the development of various types of drug carriers.[1] The encapsulation of drugs into colloidal nanocarriers (*e.g.*, polymer nanoparticles, micelles, liposomes, *etc.*) has, indeed, resulted in intensive research and promising achievements in the last decade.[2] However, strong limitations still remain which may hamper their further translation to the clinic: (i) the "*burst release*", which corresponds to the rapid release of drugs post-administration and can be harmful to patients; (ii) the encapsulation of poorly soluble drugs, exhibiting a high tendency to crystallization and (iii) the poor drug loadings (generally a few percent) that require the use of a large amount of nanocarrier materials, which can lead to prohibitive toxicity *in vivo*.

To resolve these issues, alternative strategies derived from the prodrug[3] concept have recently been reported and hold great hope due to their ability to suppress the "*burst release*" and to enable easier and more efficient incorporation of drugs into nanocarriers. For instance, drugs can be covalently linked to amphiphilic block copolymers (mainly on the hydrophobic block that is composed of the core of the nanoparticle,[2d] at the junction of the two polymer blocks[4]), or to the side chain of water-soluble polymers.[5] In the latter case, fully water-soluble conjugates or small-size aggregates are generally formed. Additionally, it has been shown that hydrophobic polymer chains can also be grown in a controlled fashion from drugs, leading to either hydrophobic polymer prodrugs further stabilized by PEG-based surfactants in the case of hydrophobic drugs,[6] or amphiphilic polymer prodrugs that can self-assemble into nanoparticles when the drug is hydrophilic.[7] In the past few years, a novel approach has emerged using squalene (Sq) – a lipidic precursor in the biosynthesis of cholesterol widely distributed in nature – as a building block for the synthesis of drug–Sq conjugates that can self-assemble in aqueous solution to form nanoassemblies with high drug payloads (~50 wt%).[8] This approach has been applied to various drugs and has led to promising results *in vivo* against several pathologies.[9] However, this novel system urgently requires an efficient targeting strategy that would enhance nanoparticle internalization by cancer cells *via* a receptor-mediated mechanism, thus avoiding potential side effects often faced when using passive drug delivery strategies.

Herein, we report an efficient and simple strategy to conceive multifunctional Sq-based nanoparticles (*i.e.*, therapeutic, fluorescent and targeted) based on the co-self-assembly of the different Sq-based functional components (Scheme 1), that is: (i) gemcitabine–squalene (Gem–Sq, a) owing to the demonstrated activity of Gem against a

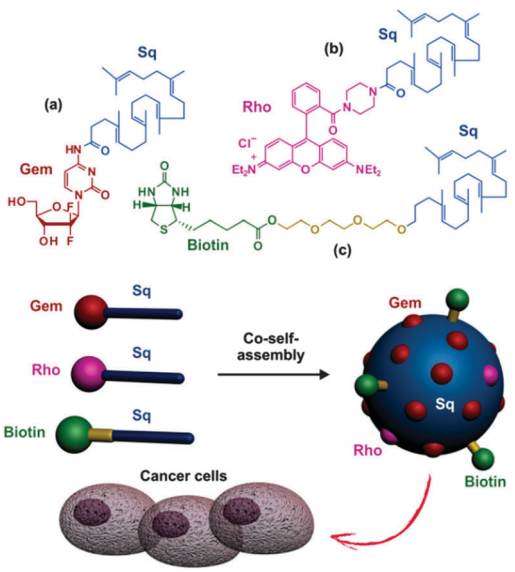

Scheme 1 Structure of gemcitabine–squalene (Gem–Sq, a), rhodamine–squalene (Rho–Sq, b) and biotin–squalene (Biotin–Sq, c), and their co-self-assembly to prepare multifunctional nanoparticles for cancer cell targeting.

Institut Galien Paris-Sud, Université Paris-Sud, UMR CNRS 8612, Faculté de Pharmacie, 5 rue Jean-Baptiste Clément, F-92296 Châtenay-Malabry Cedex, France.
E-mail: julien.nicolas@u-psud.fr; Fax: +33 1 46 83 59 46; Tel: +33 1 46 83 55 11

† Electronic supplementary information (ESI) available: Experimental details, biological activity and endocytosis in the presence of inhibitors. See DOI: 10.1039/c3cc47427e

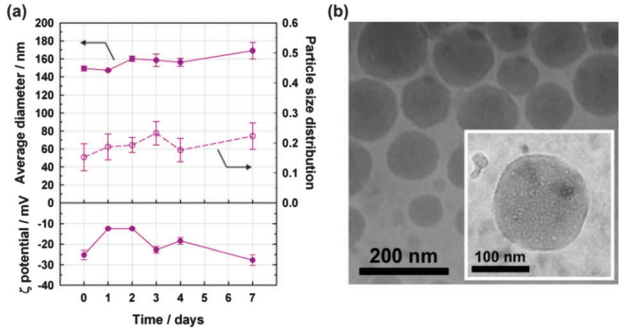

Fig. 1 Evolution of the average diameter, the particle size distribution and the zeta (ζ) potential with time (a), and cryogenic transmission electron microscopy images (b) of Gem–Sq/Biotin–Sq/Rho–Sq (86 : 9 : 5 wt%) multifunctional nanoparticles **N1***.

wide range of solid tumors;[10] (ii) rhodamine–squalene (Rho–Sq, b) due to advantageous properties of Rho (*e.g.*, high water solubility, good photostability, *etc.*) and the retained fluorescence emission at a broad range of pH of its tertiary amide derivative;[11] and (iii) biotin–squalene (Biotin–Sq, c) in order to selectively target cancer cells *via* biotin receptors overexpressed at the surface of many cancer cells.[12]

Rho–Sq was simply achieved in 90% yield by direct acylation of the piperazine-functionalized rhodamine B[11] with the chloroformate mixed anhydride of trisnor-squalenic acid.† On the other hand, Biotin–Sq was obtained from conjugation of biotin to trisnorsqualenol through a short hydrophilic triethylene glycol linker (to promote surface ligand display from the resulting nanoparticles) *via* Mitsunobu reaction.†

Multifunctional nanoparticles **N1*** were prepared by co-self-assembly of Gem–Sq, Biotin–Sq and Rho–Sq (86 : 9 : 5 wt%) in aqueous solution *via* the nanoprecipitation technique. The average diameter, D_z, was 149 ± 3 nm with a narrow particle size distribution (PSD) of ~0.15, and a zeta (ζ) potential value of −25 ± 3 mV. Their colloidal stability was assessed over a period of at least 7 days, during which little variations in their colloidal characteristics were noticed (Fig. 1a). Cryogenic-transmission electron microscopy (Cryo-TEM) showed spherical morphologies and average diameters in good agreement with DLS data (Fig. 1b). Interestingly, a thorough inspection of Cryo-TEM images showed internal organization of the nanoparticles, similarly to what has been previously observed with Gem–Sq nanoassemblies[8b] (see the inset in Fig. 1b).

Three cancer cell lines; human breast adenocarcinoma cells (MCF7), murine lung cancer cells (M109) and human cervix carcinoma cells (HeLa), which overexpress biotin receptors,[12,13] were chosen to evaluate the tumor targeting ability of the multifunctional nanoparticles **N1*** and compared to non-biotinylated Gem–Sq/Rho–Sq nanoparticles **N1** (D_z = 120 nm, PSD = 0.19). After incubation at different time intervals, the cells were collected for analysis of rhodamine B fluorescence by flow cytometry. The results showed a higher cell fluorescence intensity of all three cell lines when biotin-decorated nanoparticles **N1*** were employed, as opposed to the treatment with **N1** (Fig. 2a–c). This demonstrated the surface availability of biotin and the effectiveness of the targeting. When incubation was achieved for 4 h at 4 °C, the cell fluorescence intensity of all the three cell lines dramatically decreased down to very low values with both types of nanoparticles (Fig. 2d), suggesting internalization rather governed by endocytosis.

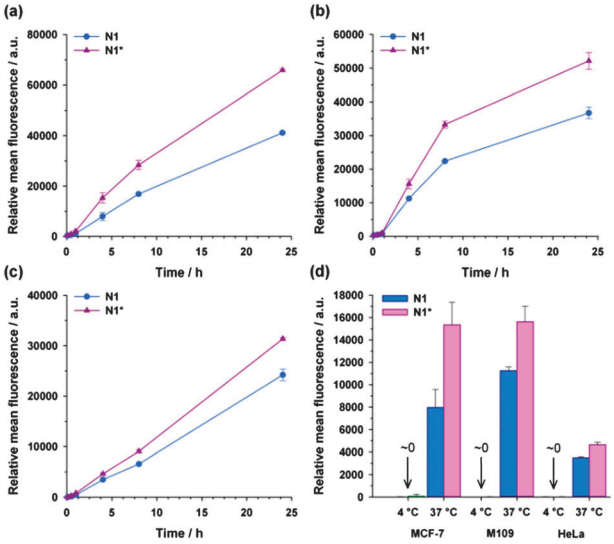

Fig. 2 Kinetics of cell capture of non-functionalized (Gem–Sq/Rho–Sq) **N1** and biotin-functionalized (Gem–Sq/Biotin–Sq/Rho–Sq) **N1*** nanoparticles in MCF7 (a), M109 (b) and HeLa (c) cells. Fluorescence of cells after incubation of MCF7, M109 and HeLa cells with nanoparticles **N1** and **N1*** for 4 h at 4 °C or 37 °C (d).

The use of specific endocytosis inhibitors (chlorpromazine, filipin III and amiloride, respectively, associated with clathrin-mediated endocytosis, caveolae-mediated endocytosis and macropinocytosis)[14] suggested that the biotinylated nanoparticles were internalized by endocytosis; clathrin and caveolae-mediated endocytotic pathways being both involved (Fig. S2).† Conversely, non-functionalized nanoparticles were not affected by endocytosis blockers, in agreement with previous literature.[15]

Importantly, in order to demonstrate the integrity of the nanoparticles during *in vitro* experiments (*i.e.*, the absence of colloidal disassembly that would split up Rho–Sq, Gem–Sq and Biotin–Sq), a similar experiment was performed with the double fluorescence labelling by using Rho–Sq and Chol–BODIPY (Table S1).† Incubation of HeLa cells with the resulting dual fluorescent nanoparticles; either targeted **N2*** (Gem–Sq/Biotin–Sq/Rho–Sq/Chol–BODIPY) or **N2** (Gem–Sq/Rho–Sq/Chol–BODIPY), was monitored by flow cytometry through both fluorescence channels associated with rhodamine B and BODIPY. Whereas Rho–Sq/Chol–BODIPY dyes alone (**N3**) resulted in poor cell capture, nanoparticles **N2*** and **N2** led to similar cell internalization patterns two-by-two, whatever the fluorescence channel (*i.e.*, by following each dye individually) (Fig. S1).† Moreover, the improved internalization, at 37 °C, of biotin-functionalized nanoparticles **N2*** compared to non-targeted counterparts **N2** was confirmed for both channels. At 4 °C, very low cell internalization was again noted.

Additionally, confocal microscopy investigation showed that multifunctional nanoparticles **N2*** are localized intracellularly as endocellular and perinuclear fluorescent spots, suggesting an endo-lysosomal distribution (Fig. 3). Noteworthy is the fact that the nearly perfect co-localization of the two fluorochromes, as attested by the overlay of the red and green fluorescence channels, suggested that the nanoparticles are likely to be still intact after 24 h of incubation.

In order to assess the therapeutic effect of the targeted Sq-based nanoparticles **N1***, they were then tested for their *in vitro* anticancer

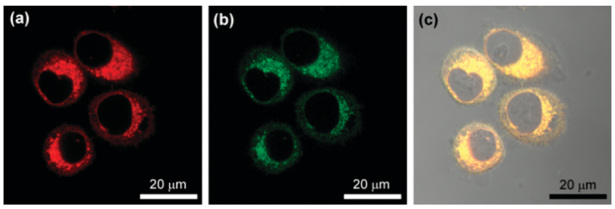

Fig. 3 Confocal microscopy images [red (Rho, a) and green (BODIPY, b) fluorescence images] and merge of red and green fluorescence images with the Nomarski image (c) after a 24 h incubation of HeLa cells with dual fluorescent Gem–Sq/Biotin–Sq/Rho–Sq/Chol–BODIPY **N2*** nanoparticles.

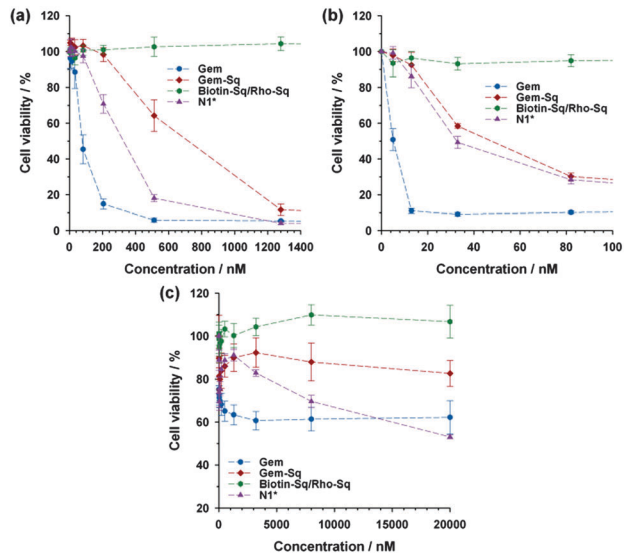

Fig. 4 Viability assay (MTT test) on HeLa (a), M109 (b) and MCF-7 (c) cells with increasing concentrations of free Gem, Gem–Sq nanoparticles **N4**, Biotin–Sq/Rho–Sq nanoparticles **N5** and nanoparticles **N1***.

activity on HeLa, M109 and MCF7 cancer cells by means of the MTT assay and compared to free Gem, Gem–Sq nanoparticles **N4** (D_z = 140 nm, PSD = 0.14) and control Biotin–Sq/Rho–Sq nanoparticles **N5** (see Table S1).† While control nanoparticles **N5** showed no cytotoxicity, targeted nanoparticles **N1*** exhibited superior anticancer activity for all three cell lines compared to Gem–Sq nanoparticles (Fig. 4). Although improvement with M109 cells was rather modest, higher cytotoxicity was observed on HeLa and MCF7 cells. For instance, IC_{50} of targeted nanoparticles **N1*** was 330 ± 12 nM for HeLa cells, whereas Gem–Sq nanoparticles displayed an IC_{50} value of 710 ± 42 nM. This shows that biotin-functionalized nanoparticles were able to enter cancer cells more efficiently, likely *via* biotin receptors, than non-functionalized nanoparticles. The observation that nanoparticles were less cytotoxic than free Gem was not surprising, due to their prodrug nature (*i.e.*, hydrolysis of the amide bond between Sq and Gem must occur to release the active Gem), with however IC_{50} values remaining in the nanomolar range. Note that the small amounts of Biotin–Sq and Rho–Sq in **N1*** are unlikely to alter the Gem release from Gem–Sq nanoparticles in biological media.[8a]

For the first time, therapeutic, fluorescent and targeted nanoparticles based on the naturally occurring Sq, using biotin as a cancer cell recognition ligand and rhodamine as a fluorescent moiety, have been prepared. The method is very simple and relies on the concomitant self-assembly of the different Sq-based building blocks to furnish stable multifunctional nanoparticles. They demonstrated improved internalization in different cancer cell lines as well as greater anticancer activity than non-functionalized Gem–Sq nanoparticles. This approach could be easily applied to other anticancer drugs (*e.g.*, nucleoside analogues, antifolic acid compounds, *etc.*), fluorescent dyes or biologically active ligands (*e.g.*, folic acid, anisamide, small peptidic sequences, *etc.*). Therefore, it paves the way to the design of various multifunctional Sq-based nanoparticles simply by changing the nature of the functional moiety linked to the Sq.

The authors thank V. Nicolas (Plateforme Imagerie Cellulaire, IFR 141) for help with the CLSM. The research leading to these results received funding from the European Research Council under the European Community's Seventh Framework Programme FP7/2007-2013 (Grant Agreement No. 249835). The PhD training program in France of the University of Science and Technology of Hanoi is acknowledged for the financial support provided to D.T.B. The authors also thank the CNRS for financial support.

Notes and references

1 O. C. Farokhzad and R. Langer, *ACS Nano*, 2009, **3**, 16.
2 (*a*) M. Elsabahy and K. L. Wooley, *Chem. Soc. Rev.*, 2012, **41**, 2545; (*b*) V. Torchilin, *Pharm. Res.*, 2007, **24**, 1; (*c*) A. Samad, Y. Sultana and M. Aqil, *Curr. Drug Delivery*, 2007, **4**, 297; (*d*) J. Nicolas, S. Mura, D. Brambilla, N. Mackiewicz and P. Couvreur, *Chem. Soc. Rev.*, 2013, **42**, 1147.
3 A. Albert, *Nature*, 1958, **182**, 421.
4 F. Bensaid, O. Thillaye du Boullay, A. Amgoune, C. Pradel, L. Harivardhan Reddy, E. Didier, S. Sablé, G. Louit, D. Bazile and D. Bourissou, *Biomacromolecules*, 2013, **14**, 1189.
5 (*a*) J. Kopeček and P. Kopečková, *Adv. Drug Delivery Rev.*, 2010, **62**, 122; (*b*) R. Duncan, *Nat. Rev. Cancer*, 2006, **6**, 688; (*c*) M. J. Vicent and R. Duncan, *Trends Biotechnol.*, 2006, **24**, 39.
6 (*a*) R. Tong and J. Cheng, *Angew. Chem., Int. Ed.*, 2008, **47**, 4830; (*b*) R. Tong and J. Cheng, *J. Am. Chem. Soc.*, 2009, **131**, 4744.
7 (*a*) S. Harrisson, J. Nicolas, A. Maksimenko, D. T. Bui, J. Mougin and P. Couvreur, *Angew. Chem., Int. Ed.*, 2013, **52**, 1678; (*b*) D. T. Bui, A. Maksimenko, D. Desmaele, S. Harrisson, C. Vauthier, P. Couvreur and J. Nicolas, *Biomacromolecules*, 2013, **14**, 2837.
8 (*a*) P. Couvreur, B. Stella, L. H. Reddy, H. Hillaireau, C. Dubernet, D. Desmaële, S. Lepêtre-Mouelhi, F. Rocco, N. Dereuddre-Bosquet, P. Clayette, V. Rosilio, V. Marsaud, J.-M. Renoir and L. Cattel, *Nano Lett.*, 2006, **6**, 2544; (*b*) P. Couvreur, L. H. Reddy, S. Mangenot, J. H. Poupaert, D. Desmaele, S. Lepetre-Mouelhi, B. Pili, C. Bourgaux, H. Amenitsch and M. Ollivon, *Small*, 2008, **4**, 247.
9 (*a*) J. L. Arias, L. H. Reddy, M. Othman, B. Gillet, D. Desmaële, F. Zouhiri, F. Dosio, R. Gref and P. Couvreur, *ACS Nano*, 2011, **5**, 1513; (*b*) L. H. Reddy, H. Khoury, A. Paci, A. Deroussent, H. Ferreira, C. Dubernet, X. Decleves, M. Besnard, H. Chacun, S. Lepetre-Mouelhi, D. Desmaele, B. Rousseau, C. Laugier, J.-C. Cintrat, G. Vassal and P. Couvreur, *Drug Metab. Dispos.*, 2008, **36**, 1570; (*c*) L. H. Reddy, P.-E. Marque, C. Dubernet, S.-L. Mouelhi, D. Desmaele and P. Couvreur, *J. Pharmacol. Exp. Ther.*, 2008, **325**, 484; (*d*) N. Sémiramoth, C. D. Meo, F. Zouhiri, F. Saïd-Hassane, S. Valetti, R. Gorges, V. Nicolas, J. H. Poupaert, S. Chollet-Martin, D. Desmaële, R. Gref and P. Couvreur, *ACS Nano*, 2012, **6**, 3820; (*e*) F. Bekkara-Aounallah, R. Gref, M. Othman, L. H. Reddy, B. Pili, V. Allain, C. Bourgaux, H. Hillaireau, S. Lepetre-Mouelhi, D. Desmaele, J. Nicolas, N. Chafi and P. Couvreur, *Adv. Funct. Mater.*, 2008, **18**, 3715.
10 L. W. Hertel, G. B. Boder, J. S. Kroin, S. M. Rinzel, G. A. Poore, G. C. Todd and G. B. Grindey, *Cancer Res.*, 1990, **50**, 4417.
11 T. Nguyen and M. B. Francis, *Org. Lett.*, 2003, **5**, 3245.
12 G. Russell-Jones, K. McTavish, J. McEwan, J. Rice and D. Nowotnik, *J. Inorg. Biochem.*, 2004, **98**, 1625.
13 E. S. Lee, K. Na and Y. H. Bae, *Nano Lett.*, 2005, **5**, 325.
14 H. Hillaireau and P. Couvreur, *Cell. Mol. Life Sci.*, 2009, **66**, 2873.
15 L. Bildstein, V. Marsaud, H. Chacun, S. Lepetre-Mouelhi, D. Desmaele, P. Couvreur and C. Dubernet, *Soft Matter*, 2010, **6**, 5570.

